Nuclear Materials and Energy 26 (2021) 100848

Contents lists available at ScienceDirect

Nuclear Materials and Energy

journal homepage: www.elsevier.com/locate/nme

Experimental observations and modelling of radiation asymmetries during N_2 seeding in LHD

B.J. Peterson [a,b], G. Kawamura [a,b], P.L. van de Giessen [c], K. Mukai [a,b], H. Tanaka [d], R. Sano [e], S. N. Pandya [f], S.Y. Dai [g], S. Masuzaki [a,b], T. Akiyama [a,h], M. Kobayashi [a,b], M. Goto [a,b], G. Motojima [a,b], R. Sakamoto [a,b], N. Ohno [d], T. Morisaki [a,b], J. Miyazawa [a,b], the LHD Experiment Group [a]

[a] National Institute for Fusion Science, Toki, Gifu-ken 509-5292, Japan
[b] Graduate University for Advanced Studies SOKENDAI, Hayama 240-0163, Japan
[c] Eindhoven University of Technology, 5612 AZ Eindhoven, the Netherlands
[d] Graduate School of Engineering, Nagoya Univ., Nagoya, Aichi-ken 464-8603, Japan
[e] National Institutes for Quantum and Radiological Sci. and Tech., Naka 311-0193, Japan
[f] Institute for Plasma Research, Gandhinagar, Gujarat 382 428, India
[g] School of Physics, Dalian University of Technology, Dalian 116024, PR China
[h] General Atomics, San Diego, CA, USA

ARTICLE INFO

Keywords:
Impurity seeding
Bolometer
Radiation
Plasma
Magnetic fusion

ABSTRACT

N_2 gas has been seeded in the Large Helical Device (LHD) to reduce the divertor heat load through enhanced radiation. Radiation is observed by two imaging bolometers, viewing the same poloidal cross-section from top and bottom ports, at a location which is 36° toroidally removed from the N_2 gas puff nozzle located at the bottom of the machine. During N_2 seeding, these measurements both confirm that additional radiation from the outboard side is coming exclusively from the top of the cross-section, indicating up/down asymmetry, which is also reproduced by modelling with EMC3-EIRENE using a half torus model. In addition, a toroidally localized, magnetic field direction-dependent radiation enhancement is observed with N_2 seeding, but is not reproducible by the model.

1. Introduction

Radiative cooling by impurity gas seeding will be an important tool for the reduction of heat load to the divertor of a fusion reactor. Candidate impurity gasses include N_2, Ne, Ar and Kr, with lighter gasses being used to cool the lower temperature plasma in the divertor and higher Z gasses used to cool the higher temperature plasma near and inside the last closed flux surface (LCFS) [1]. However, the use of higher Z impurities such as Ar or Kr is accompanied by the degradation of confinement presumably due to the radiative cooling inside the LCFS [2,3]. In the Large Helical Device (LHD) radiative cooling through impurity seeding with Ne and Kr have been demonstrated [3–5]. Toroidally asymmetric divertor particle flux distributions have been reported in LHD during N_2 seeding with the magnetic axis set to $R_{axis} = 3.6$ m [6], which were in qualitative agreement with modelling for the low recycling case [7]. In a tokamak, toroidal asymmetries during seeding of N_2 have been studied both experimentally and through modelling [8].

Recently, new tools have become available which are useful in understanding the complicated radiative structures existing particularly in three dimensional (3D) magnetic geometries in helical devices and magnetically perturbed tokamaks. On the experimental side, these include the InfraRed (IR) imaging Video Bolometer (IRVB) [9,10], which produces an absolutely calibrated image of the line-integrated radiation from the plasma. On the modelling side, the 3D edge plasma transport code EMC3-EIRENE [11,12] is a powerful means for modelling the radiated power distribution for a given impurity gas in the complicated edge plasmas of helical devices and magnetically perturbed tokamaks. This code has recently been extended to the divertor leg region in LHD [13]. Through the utilization of a synthetic diagnostic technique, the modelling data can be directly compared to the experimental images to provide a physical understanding of the complicated 3-D structure of the impurity radiation. Additionally, resistive bolometers located at

E-mail address: peterson@LHD.nifs.ac.jp (the LHD Experiment Group).

https://doi.org/10.1016/j.nme.2020.100848
Received 31 July 2020; Received in revised form 8 October 2020; Accepted 11 November 2020
Available online 1 December 2020
2352-1791/© 2020 The Author(s). Published by Elsevier Ltd. This is an open access article under the CC BY-NC-ND license (http://creativecommons.org/licenses/by-nc-nd/4.0/).

different toroidal angles can give a local estimate of the total radiated power that can be used to study the toroidal asymmetries [14].

2. Experimental procedure and modelling technique

2.1. Experimental procedure

All experiments were carried out on LHD, which is an l = 2, ten field period (m = 10) Heliotron type device utilizing a pair of helical coils and 3 pairs of vertical field coils to confine the plasma. The magnetic axis positions used in these experiments were $R_{axis} = 3.6$ m and 3.9 m. Outer ports are designated 1-O through 10-O corresponding to the field period. Upper/lower ports are designated 1.5-U/L through 10.5-U/L since they are one half field period offset from the outer ports due to the helical coils. The plasmas were neutral beam injection (NBI) heated using tangentially injected beams. N_2 gas was puffed from Ports 3.5-L, 5.5-L and 9.5-L. Total radiated power data shown in the shot summary is measured by a single wide-angle resistive bolometer located at the 3-O Port. In addition, resistive bolometer arrays located at the 8-O and 6.5-L ports are used to study toroidal asymmetries.

2.2. Imaging bolometers

The IRVB is a diagnostic that measures an image of the total power radiated by the plasma. A thin (~2.5 μm) Pt foil blackened with graphite and exposed to the plasma through a square aperture absorbs the plasma radiation. Using the time varying temperature distribution of the foil, measured by an infrared camera, the 2D heat diffusion equation of the foil is used to solve for the radiated power, *P*, absorbed by the foil. The IRVBs used in this study were installed on the 6.5-U and 6.5-L ports. CAD images of the fields of view (FoVs) are shown in Fig. 1. The lower port IRVB has 20 (poloidal) × 28 (toroidal) pixels and the upper port IRVB has 18 (poloidal) × 24 (toroidal) pixels. The time resolution for both is 20 ms. LHD poloidally has a double null divertor structure that rotates poloidally with increasing toroidal angle. Therefore, the divertor x-points have a helical shape and their trajectories in the FoVs of the IRVBs are shown by dashed lines in Fig. 1.

2.3. EMC3-EIRENE modeling and synthetic image calculation

The EMC3-EIRENE model used in this study includes the divertor leg region of the plasma [13]. The synthetic images of radiated power density at the bolometer foil are calculated from the three dimensional (3D) radiated power density predicted by the EMC3-EIRENE code using ray tracing.

Two types of N_2 recycling cases are modelled to account for uncertainties in assuming the recycling coefficient for N_2. One, referred to as the 100% recycling model, uses a neutral nitrogen source on the divertor plates to simulate the release of the gas due to surface recombination. Gas puff nozzles are not in use in this case because there is no loss of nitrogen. Therefore, the plasmas in every helical section are identical with 100% recycling by definition. The other model, referred to as the 0% recycling model, uses gas puff nozzles and no surface recombination to simulate the quick decay of nitrogen gas pressure due to adsorption of nitrogen atoms onto the wall surfaces.

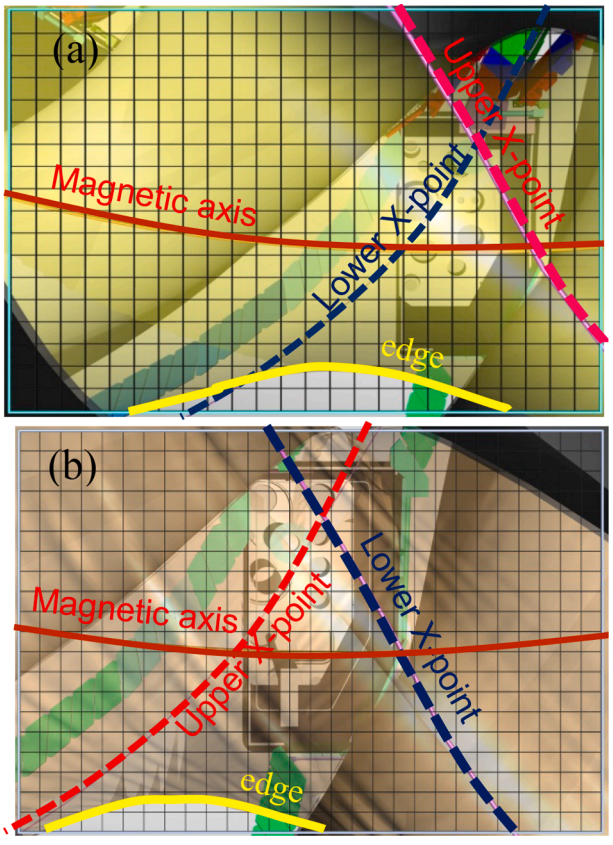


Fig. 1. CADs of (a) upper and (b) lower IRVB fields of view (with grey grid showing field of view of each bolometer pixel), Dashed lines show upper (red) and lower (blue) divertor x-point traces and solid orange lines shows magnetic axis. Inboard side (lower major radius) is at the top of figure and outboard side (higher major radius) is at the bottom of figure. The yellow line indicates the outboard edge of the plasma. (For interpretation of the references to colour in this figure legend, the reader is referred to the web version of this article.)

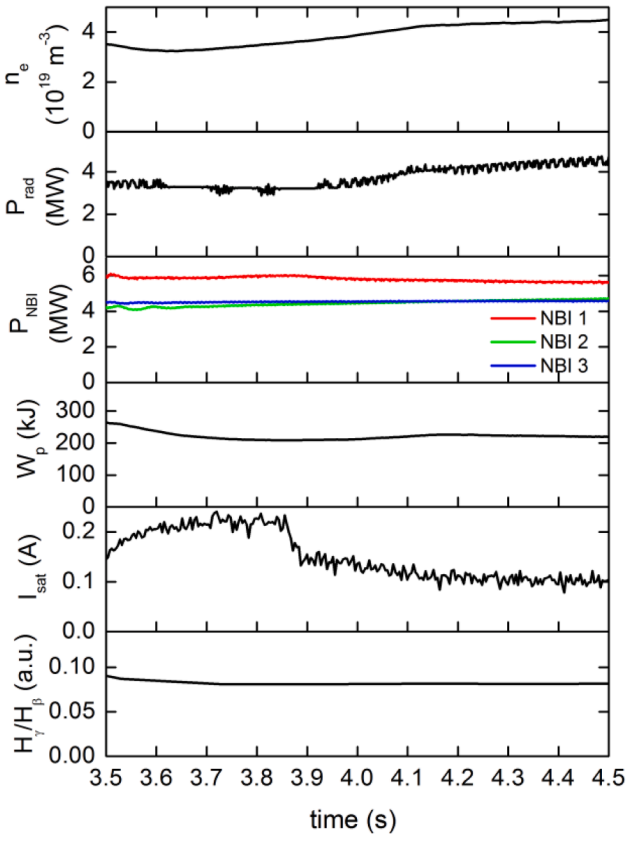


Fig. 2. Discharge summary of LHD shot #123366 with N_2 puffing from 3.8 s to 4.8 s.

3. N_2 seeding experiments

3.1. Evolution of fundamental parameters

N_2 seeding experiments were carried out as shown in the discharge summary shown in Fig. 2. N_2 was puffed from 3.8 to 4.8 s, which resulted in an ~20% increase in the radiated power and a decrease in the divertor flux. In some discharges the radiation increment (increase compared to level prior to seeding) with N_2 can be up to 100%. No change in the H_γ/H_β ratio indicates that this seeding also did not lead to detachment, but rather only to a radiative divertor condition. Stored energy remained nearly constant. The change in divertor heat flux (indicated by I_{sat}) was observed to be quasi-uniform in the case of Ne but toroidally localized in the case of N_2 [6].

3.2. Change in bolometric images with N_2 seeding

In Fig. 3 two time frames from the upper port (6.5-U) imaging bolometer are shown, one before the N_2 seeding at 3.6 s and one during the N_2 seeding at 4.4 s. Prior to the N_2 seeding (Fig. 3(a)), the radiaton is coming mainly from the upper divertor x-point region and to a lesser extent from the lower divertor x-point and outboard edge. During the N_2 seeding (Fig. 3(b)), one notes that a strong second radiation stripe on the outboard side developed along the upper helical divertor x-point trace in addition to radiation from the outboard edge region. Observation from an IRVB viewing from the 6.5-L port (see Fig. 3(c)), directly below the 6.5-U IRVB, confirms that this radiation is coming from along the upper helical divertor x-point trace and therefore is poloidally (up-down) asymmetric. Also, observations with an IRVB from the 10-O port (not shown) show no double stripe pattern indicating that the second stripe is toroidally localized.

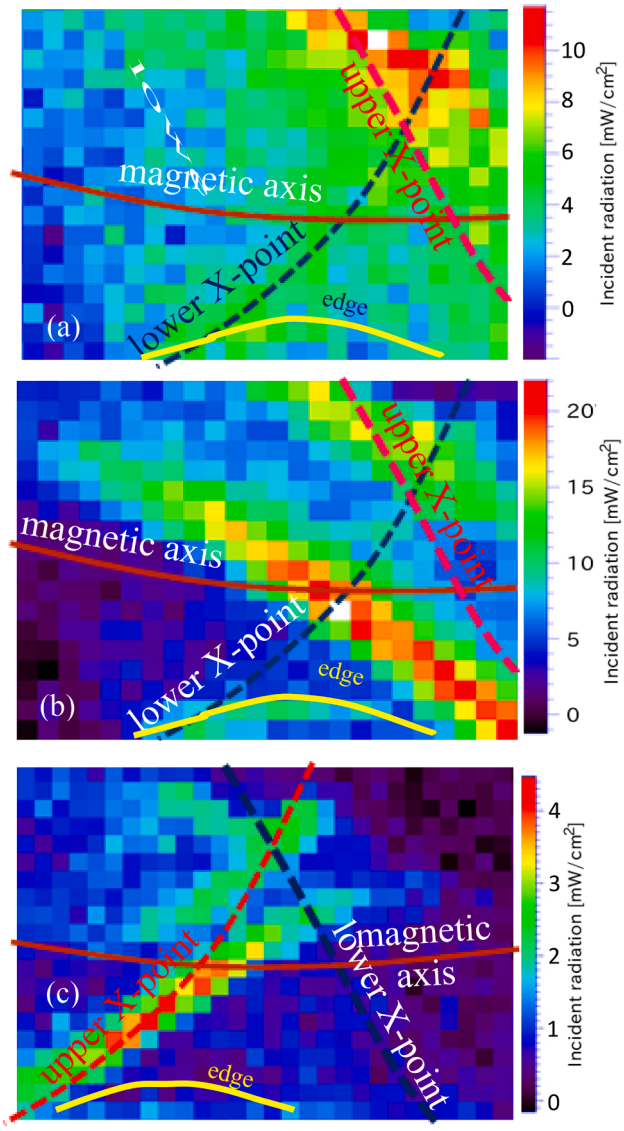


Fig. 3. Bolometric images from an LHD upper port (6.5-U) at (a) 3.6 and (b) 4.4 s and (c) from a lower port (6.5-L) at 4.4 s during shot # 123366. Dashed lines show upper (red) and lower (blue) divertor x-point traces and solid orange lines shows magnetic axis. (For interpretation of the references to colour in this figure legend, the reader is referred to the web version of this article.)

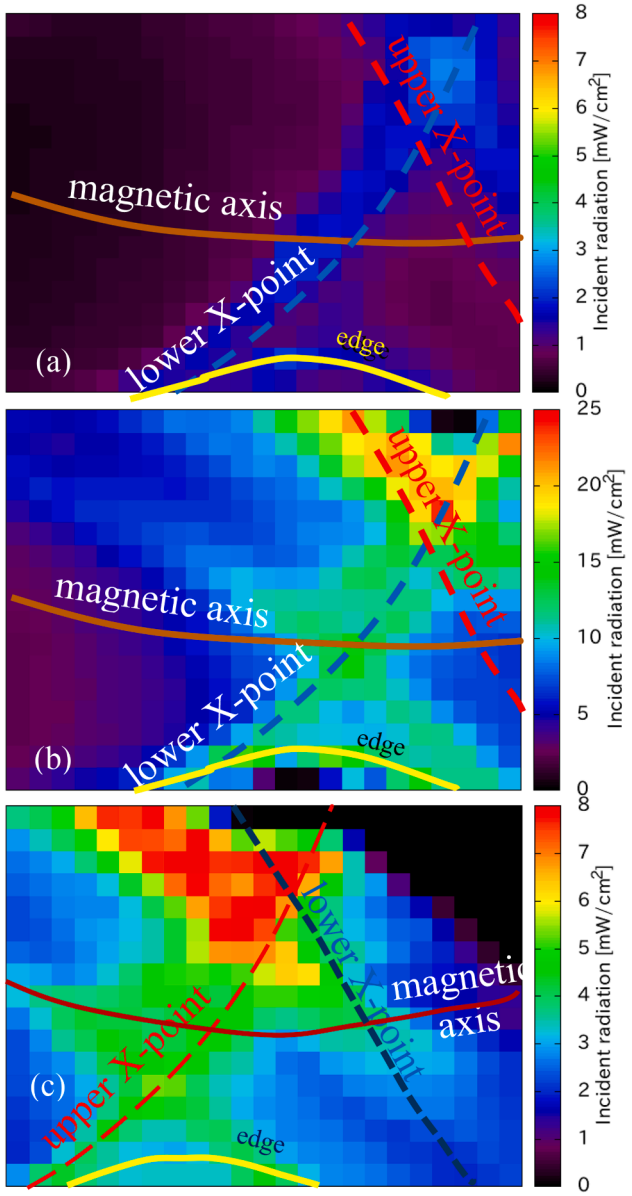


Fig. 4. Synthetic images from 18° EMC3-EIRENE for the IRVBs for 10 MW input power at 6.5-U with (a) no N_2 seeding, (b) N_2 seeding (8 MW) with 0% recycling and (c) same as (b) but at 6.5-L.

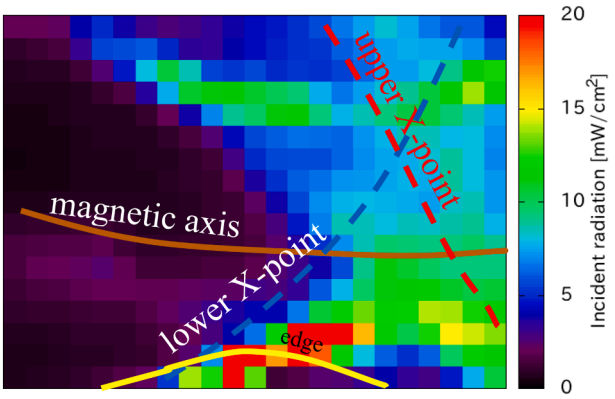


Fig. 5. Poloidal radiation profile cross-sections from a 180° (toroidal) EMC3-EIRENE model at the (a) 5.5 and (b) 6.5 port locations for N_2 seeding with 0% recycling.

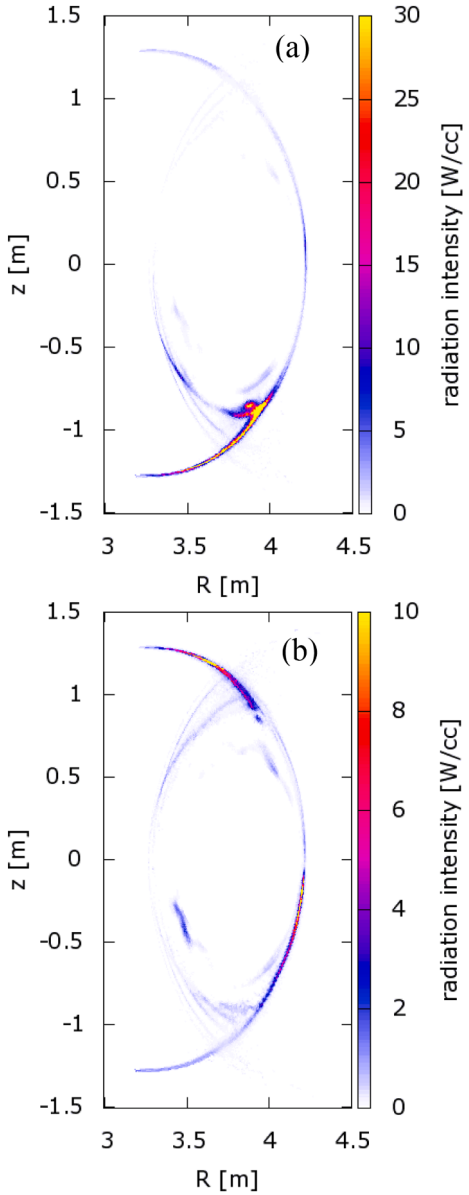


Fig. 6. Synthetic images from 180° EMC3-EIRENE for the 6.5-U IRVB for 10 MW input power with N_2 seeding (6 MW) with 0% recycling.

4. Modeling of impurity radiation during N_2 seeding

4.1. Half field period model

A half period (18° toroidally) model has been developed which is intrinsically an up/down symmetric model since it places gas puff nozzles at both the upper and lower ports. The synthetic images for this model corresponding to the experimental images in Fig. 3 are shown in Fig. 4.

One notes that the case with no N_2 seeding (Fig. 5(a)) shows the same features as the corresponding experimental image before N_2 seeding with radiation coming from the upper and lower divertor x-points and the outboard edge. Absolute values are about half of the experimental levels. In the cases with N_2 seeding the outboard stripe appears, albeit weaker and shorter in length than in experiment, while the absolute values are comparable to the experiment. There are no significant differences seen between the cases of 100% (not shown) and 0% recycling with N_2 seeding. Since this is an inherently up/down symmetric model, the second stripe is also seen along the lower divertor x-point trace in contrast to the experiment. In Fig. 4(c) the location of double stripes along the upper X-point agrees with the those in the experimental image (Fig. 3(c)) although they are not as bright as those along the lower X-point due to the up/down symmetry of the model.

4.2. Half torus model

A half torus (180° toroidally) model has been developed which placed the gas puff nozzle at Port 5.5-L (same as in the N_2 seeding experiment) and also at 1.5-U, due to symmetry. The results for N_2 seeding with 0% recycling, 10 MW of heating and 6 MW of N_2 radiation are seen in Fig. 5. They clearly show the poloidal (up-down) asymmetry in the radiation at the 6.5-U port resulting from the magnetic field line connection to the gas puffing location at the 5.5-L port. Also, the corresponding synthetic image for the 6.5-U IRVB is shown in Fig. 6. Good qualitative agreement between the experimental and synthetic images is seen for the inboard stripe. Also, evidence of the outboard stripe is seen in the synthetic image, but is weaker and has a more segmented structure than what is seen in the experiment. The radiated power from the outboard edge is relatively stronger than that seen in the experiment.

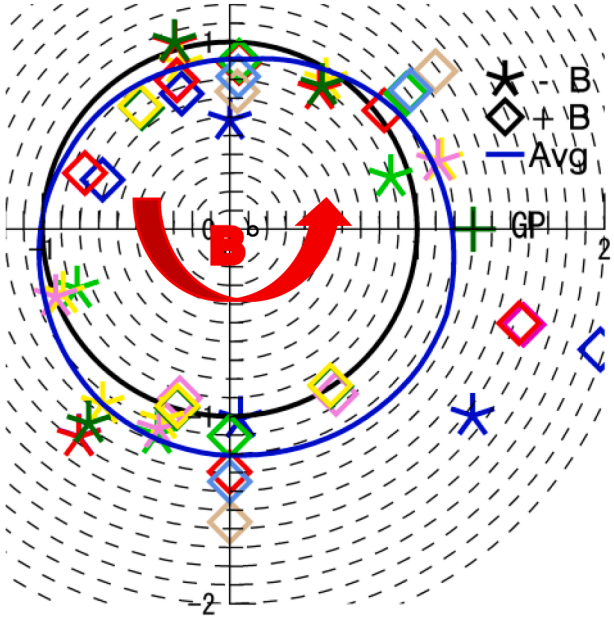


Fig. 7. Local relative enhancement of total radiated power versus toroidal angle due to impurity seeding at gas puff (GP) valve at 0° (+) for N_2. The black line is the normalized total radiated power and symmetric reference.

5. Toroidal asymmetry and B polarity dependence

When the magnetic field direction is reversed, the poloidal asymmetry observed in the outboard stripe of the radiation images in Fig. 3 (b) and (c) disappears. This magnetic field direction-dependent, toroidally asymmetric radiation enhancement due to impurity seeding is further investigated by plotting versus toroidal angle in Fig. 7 the local enhancement of the radiation relative to the enhancement in the global total radiation as observed by the resistive bolometer arrays in LHD. The data is rotated toroidally with respect to the gas seeding port in order to place all of the seeding ports at the 0° toroidal angle (indicated by green cross) and then data for positive magnetic field direction are flipped toroidally with respect to the seeding port (0°). Radiation enhancement due to N_2 seeding is seen to be toroidally localized peaking at 60° toroidally from the seeding port in the direction opposite the magnetic field. The parameter range is $4–7 \times 10^{19}\,m^{-3}$ for peak density and 2–3.2 keV for peak electron temperature.

6. Discussion

A poloidal (up-down) asymmetry due to a toroidally localized radiation zone has been observed during N_2 seeding in LHD. The observation of this localized radiation enhancement during N_2 seeding is attributed to two conditions. The first is the reduced recycling of N_2 presumably due to its reactivity. The second condition is the short connection length between the gas puff location at port 5.5-L and the observed radiation at port 6.5-U. This effect is well demonstrated by the 180° model as seen in Fig. 6. However, we only see weak evidence of the outboard radiation zone in the case of the 180° model. In addition, the experimentally observed enhancement in radiation due to N_2 seeding is toroidally localized at a location dependent on the magnetic field polarity which suggests the role of drifts that, however, cannot be modelled by EMC3-Eirene.

Several deficiencies in the EMC3-EIRENE model may be preventing it from correctly predicting the location of the outboard radiation zone. The first is the limited minor radial extent of the model which only extends from the plasma edge to near the last closed flux surface (LCFS). If the outboard radiation zone is inside the LCFS as the triangulation suggests then it would not appear in the model. However, it is hard to understand how such a localized radiation pattern could appear inside the LCFS. Another deficiency is the density profile used in the model. While the experimental profiles are typically hollow for this magnetic configuration, the model uses a peaked profile due to the lack of an outward convection term. Therefore, the minor radially inner part of the model may not correctly reflect the impurity radiation distribution.

CRediT authorship contribution statement

B.J. Peterson: Conceptualization, Methodology. **G. Kawamura:** . **P. L. van de Giessen:** . **K. Mukai:** . **H. Tanaka:** . **R. Sano:** . **S.N. Pandya:** . **S.Y. Dai:** . **S. Masuzaki:** Supervision. **T. Akiyama:** . **M. Kobayashi:** . **M. Goto:** . **G. Motojima:** . **R. Sakamoto:** . **N. Ohno:** Supervision. **T. Morisaki:** Supervision. **J. Miyazawa:** . **:** .

Declaration of Competing Interest

The authors declare that they have no known competing financial interests or personal relationships that could have appeared to influence the work reported in this paper.

Acknowledgement

This work was done with the support of National Institute for Fusion Science research grant NIFS15ULHH026.

References

[1] A. Kallenbach, et al., Plasma Phys. Control. Fusion 55 (2013), 124041.
[2] M.L. Reinke, et al., J. Nucl. Mater. 415 (2011) S340.
[3] K. Mukai, et al., Nucl. Fusion 55 (2015), 083016.
[4] S. Masuzaki, et al., J. Nucl. Mater. 438 (2013) S133.
[5] K. Mukai, et al., Plasma Fusion Res. 15 (2020), 140205.
[6] H. Tanaka, et al., Nucl. Mater. Energy 12 (2017) 241.
[7] G. Kawamura, et al., Plasma Phys. Contr. Fusion 60 (2018), 084005.
[8] J.D. Lore, et al., J. Nucl. Mater. 463 (2015) 515.
[9] B.J. Peterson, Rev. Sci. Instrum. 71 (2000) 3696.
[10] B.J. Peterson, et al., Rev. Sci. Instrum. 74 (2003) 2040.
[11] Y. Feng, et al., J. Nucl. Mater. 266–269 (1999) 812.
[12] D. Reiter, et al., Fusion Sci. Tech. 47 (2005) 172.
[13] G. Kawamura, et al., Contrib. Plasma Phys. 54 (2014) 437.
[14] P.L. van de Giessen, et al., submitted to Rev. Sci. Instrum.